CaH Rydberg Series, Oscillator Strengths and Photoionization Cross Sections from Molecular Quantum Defect and Dyson Orbital Theories

A. M. Velasco and C. Lavín

Departamento de Química Física, Universidad de Valladolid, 47005 Valladolid, Spain

Manuel Díaz-Tinoco and J. V. Ortiz*

Department of Chemistry and Biochemistry, Auburn University, Auburn AL 36849-5312, U. S. A.

Abstract

In this work, electron-propagator methods are applied to the calculation of the ionization potential and vertical excitation energies for several Rydberg series of the CaH molecule. The present calculations cover more highly excited states than those previously reported. In particular, excitation energies for ns (n>5), np (n>5), nd (n>4) and nf Rydberg states are given. Oscillator strengths for electronic transitions involving Rydberg states of CaH, as well as photoionization cross sections for Rydberg channels, also have been determined by using the Molecular Quantum Defect Orbital approach. Good agreement has been found with the scarce comparative data that are available for oscillator strengths. To our knowledge, predictions of photoionization cross sections from the outermost orbital of CaH are made here for the first time. A Cooper minimum and mixed atomic orbital character in some of the Dyson orbitals are among the novel features of these present calculations.

*ortiz@auburn.edu

Introduction

Calcium monohydride has been a molecule of considerable interest to spectroscopists, theoreticians and astrophysicists since it was first identified in the spectra of sunspots [1,2] and M dwarf stars [3]. Ever since, several bands of CaH have been detected in cool brown dwarfs, where high abundances of this molecule have been recorded [4,5,6]. More recently, the chemical abundance of CaH in Kapteyn's Star [6] and in T dwarfs have been determined [7,8]. Moreover, CaH is thought to be a relevant repository of gas-phase metal atoms [9] because its spectrum is present in a variety of interstellar environments. Because molecular absorption is the most important opacity source in cool, stellar atmospheres [10], spectroscopic data on electronic, vibrational, and rotational transitions of CaH are of great importance. On the other hand, hundreds of extrasolar planets have been discovered in the last decades. The analysis of the composition and physical features of exoplanets, where CaH is thought likely to be relevant, requires copious spectroscopic data, most of which are difficult to obtain from laboratory experiments [11]. Theoretical methods that are both accurate and efficient for predicting spectral properties could make a valuable contribution to knowledge of the spectroscopy of the CaH molecule.

The spectrum of CaH has been the subject of many experimental and theoretical studies since it was first photographed by Olmsted in emission [1]. A summary of spectroscopic and astrophysical studies of CaH has been provided by Shayesteh et al. [12] and more recently by Yadin et al. [13]. The compiled studies included those focused on the determination of spectroscopic properties, potential energy curves and dipole moments for the ground and some low-lying electronic states. However, in spite of numerous studies on the CaH spectrum, available data are limited to its low-lying states. Thus, it is the aim of the present work to supply new molecular data for calcium

monohydride directly associated with electronic transition properties involving Rydberg states. We have inferred vertical excitation energies of ns, np, nd and nf Rydberg series of CaH in the 1.8-5.5 eV energy range from differences of electron affinities of CaH^+ calculated with electron-propagator methods. [14,15] Because this approach also yields Dyson orbitals that connect the ground state of CaH^+ to ground and excited states of CaH, atomic contributions to the Rydberg orbitals may be identified.

Studies on electronic transition intensities of CaH are limited to some low-lying states despite the need for more general data in developing reliable atmospheric models of cool stars and extrasolar giant planets [16]. Barbuy et al. [17] have derived oscillator strengths for the $A^2\Pi$-$X^2\Sigma$ and $B^2\Sigma$-$X^2\Sigma$ systems from a comparison of their lines obtained with model atmospheres and the observed spectra. Otherwise, Bruna and Grein [18] have calculated oscillator strengths for several transitions of CaH using a single-reference *ab initio* method. Their study is limited to transitions involving 5p, 4d and 5s Rydberg states. Hence, another goal of the present study is to provide intensities of electronic transitions from the ground state to higher excited states including the continuum. Considering the good performance of the Molecular Quantum Defect Orbital (MQDO) method, which is semi-empirical in character, in calculations of one-photon transition intensities involving Rydberg states and its reliability in previous applications [19,20], including another metal hydride (BeH) [21], we have used this approach to determine oscillator strengths and photoionization cross sections of the CaH molecule. The vertical excitation energies calculated with electron-propagator methods have been used as parameters in the MQDO method. In previous works [22,23], *ab initio* electron-propagator energy data and the MQDO oscillator strengths calculated with them have proved to be consistent with the most accurate *ab initio* calculations. In this work, we have determined oscillator strengths for dipole-allowed transitions from the $X^2\Sigma^+$ ground

state to $np^2\Sigma^+$ and $np^2\Pi$ Rydberg series. Our results have been compared with the scarce comparative data available in the bibliography. For the continuum region we have estimated the photoionization cross sections for the $kp^2\Sigma^+$ and $kp^2\Pi$ Rydberg ionization channels. A Cooper minimum, which is a useful phenomenon for analyzing photoelectron dynamics [24], is found in our calculated cross sections. Cooper minima also have been observed in previous applications of the MQDO method to molecular photoionization studies [25,26]. To our knowledge neither theoretical nor experimental continuum transition intensities of CaH have been reported. In order to assess the correctness of our results, we have determined the oscillator-strength spectral density in the discrete and continuum regions and have analyzed the continuity of this property near the ionization potential.

Methods of calculation

A. Electron-propagator theory

In electron-propagator calculations, electron-binding energies and Dyson orbitals are the eigenvalues and eigenfunctions of an energy-dependent, non-local, one-electron operator that incorporates the effects of orbital relaxation and electron correlation. [14,15] For the i-th electron affinity of a cationic ground state with N-1 electrons, the corresponding Dyson orbital reads

$$\Phi_i^{\text{Dyson}}(x_1) = N^{1/2} \int \Psi_{i,\text{molecule}}(x_1,x_2,x_3\ldots,x_N)\, \Psi^*_{\text{cation}}(x_2,x_3,x_4\ldots,x_N)\, dx_2 dx_3 dx_4 \ldots dx_N, \quad (1)$$

where x_k is the space-spin coordinate of electron k. This *ab initio* approach may be systematically improved to the exact limit by incorporating more terms in the self-energy operator. In the present study, the self-energy operator is calculated in the 3+ approximation, a method that includes all third-order and many higher-order terms in the

self-energy operator through a renormalization procedure. Pole strengths, *i.e.* the norms of the Dyson orbitals, approach unity when electron correlation effects vanish. For most of the present transitions, pole strengths exceed 0.95 and validate the qualitative picture of a Rydberg state consisting of a cationic core with a diffuse orbital that resembles a hydrogenic eigenfunction. Mulliken populations of Dyson orbitals normalized to unity suffice to identify cases where there is substantial mixing of atomic orbitals with different *l* quantum numbers. A cc-pvqz basis set [27,28] augmented by even-tempered 9s, 9p, 9d and 9f diffuse functions on Ca is employed. Exponents of the latter functions are generated by successively applying a multiplicative factor of one third to the least diffuse s, p, d and f members of the Ca cc-pvqz set. The first five occupied molecular orbitals (i.e. those that are chiefly 1s, 2s or 2p Ca functions) are neglected in the calculation of the 3+ self-energy. Therefore, CaH^+ has five active occupied orbitals in the electron-propagator calculations.

Additional *ab initio* calculations in the coupled-cluster singles and doubles plus perturbative triples, or CCSD(T), approximation [29] have been performed to procure the adiabatic ionization energy of CaH: 5.627 eV. The latter datum includes zero-point energies and is used in MQDO calculations. The bond length of CaH optimized with CCSD(T), 2.0034 Å, is assumed in the electron-propagator calculations of the electron affinities of CaH^+. The first vertical electron affinity (i.e. that connecting the ground states of CaH^+ and CaH) calculated in the 3+ approximation of electron-propagator theory is 5.663 eV, with a pole strength of 0.968. (The CCSD(T) result is within 0.01 eV of the electron-propagator value.) Differences of vertical electron affinities constitute vertical excitation energies of CaH.

All ab initio calculations were performed with the development version of Gaussian. [30]

B. Molecular Quantum Defect Orbital method (MQDO)

The MQDO methodology has been previously reported in several papers [31,32] and, therefore, the major points are presented briefly here. It is based on a model one-electron Hamiltonian with a parametric potential of the form:

$$V(r) = \frac{\lambda(\lambda+1) - l(l+1)}{2r^2} - \frac{1}{r} \qquad (2)$$

where λ is a parameter, related to the quantum defect, δ, and the orbital angular moment, l, which determines the electron screening.

In the MQDO method, the wave function is expressed as a product of a radial function and an angular function. The radial part is the analytical solution of the Schrödinger equation and the angular part is a symmetry-adapted linear combination of spherical harmonics.

The absorption oscillator strength for an electronic transition between two bound states adopts the following expression:

$$f = \frac{2}{3} N(E_b - E_a) Q\{a \to b\} |R_{ab}|^2 \qquad (3)$$

and the photoionization cross-section for a transition between a bound state and a continuous state adopts this form:

$$\sigma = 2.6891 \left[\frac{1}{(n-\delta)^2} + k^2 \right] \frac{1}{2k} NQ\{a \to b\} |R_{ab}|^2 \qquad (4)$$

In both equations, $Q\{a \to b\}$ are the angular factors resulting from the angular integration, N is the number of electrons in the orbital where the transition initiates and k^2 is the kinetic energy of the free electron upon ionization in Rydberg units. R_{ab} is the radial transition

moment which has a closed-form analytical expression. This fact offers, in our view, an important computational advantage compared to *ab initio* methods.

Results and discussion

A. Transition energies

The $X^2\Sigma^+$ ground-state electronic configuration at its equilibrium geometry can be written as [core]($1\sigma^2 2\sigma$), where the highest occupied 2σ orbital is chiefly an atomic Ca 4s orbital. The present calculated absorption spectrum of CaH corresponds to vertical excitations from the ground state to states belonging to the following Rydberg series: nsσ ($^2\Sigma^+$), npσ ($^2\Sigma^+$), npπ ($^2\Pi$), ndσ ($^2\Sigma^+$), ndπ ($^2\Pi$), ndδ ($^2\Delta$), nfσ ($^2\Sigma^+$), nfπ ($^2\Pi$), nfδ ($^2\Delta$) and nfφ ($^2\Phi$). The quantum number n of the Rydberg states has been determined through a careful analysis of the quantum defects associated with each of the Rydberg series of CaH. To do this, we have taken into account the fact that the values of the quantum defect for hydrides usually are of the same magnitude as those of the corresponding atom [33]. In particular, the quantum defects for the Ca atom are about 3, 2, and 1 for the s, p and d series, respectively [34].

The presently calculated vertical excitation energies are collected in Table 1. It should be noted that the s, p, d and f denotations of the Rydberg states may be an over-simplification when mixing is present (see Q column in Table 1). For comparative purposes, in Table 2, our results for Rydberg states are displayed together with experimental values found in the literature [35,36,37]. As can be seen, a good agreement (to within ~0.15 eV) is found in most of the assignments and energy values. However, for the $B^2\Sigma^+$ state observed at 1.954 eV which was experimentally assigned to a $2\sigma \rightarrow 4p\sigma$ excitation, our calculations indicate the final state has a mixed singly-occupied orbital instead. (A Mulliken population analysis of the Dyson orbital shows 59% d and 34% p character.) The $^2\Delta$ state

at 2.461 eV may be assigned to a 2σ→3dδ transition that resembles results on a $1^2\Delta$ state identified computationally by Bruna and Grein (2.86 eV) [18] and by Leininger and Jeung (2.38 eV) [38] with configuration interaction. From our calculations, the $E^2\Pi$ and $C^2\Sigma^+$ experimentally observed states correspond to 3dπ and 5sσ Rydberg states, respectively. We also have tentatively assigned the $F^2\Sigma^+$ state observed at 4.55 eV [39] to a 2σ→6sσ Rydberg excitation.

In most cases, the pole strengths are close to unity and the Dyson orbitals are dominated by a contribution from a single, canonical, Hartree-Fock orbital. The molecular orbital picture of the Rydberg states remains qualitatively valid when the correlation effects inherent in 3+ electron-propagator calculations are considered. There are several states where the Dyson orbital exhibits considerable mixing of Ca s, p, d or f functions, but most cases have a single, dominant *l* component. Correlation and relaxation corrections to canonical Hartree-Fock orbital energies obtained in 3+ calculations decline in importance with increasing excitation energy for the cases where the pole strength is close to unity.

For low values of n, the quantum defects shown in Fig. 1 (see footnote e in Table 1) are approximately constant for a given Rydberg series and confirm the adequacy of the Gaussian basis. The sensitivity of the quantum defects to the energy values results in the anomalous behavior seen for higher n. For example, in the s series, a variation of ±0.05 eV in the 5s Rydberg state at 5.31 eV produces a change of ±0.03 in δ, whereas for the 12 s state at 5.61 eV, the same variation changes δ from -18.12 to -2.47. Addition of more diffuse Gaussian functions can be expected to provide better exponential tails in the Dyson orbitals and improved quantum defects for the higher Rydberg states.

B. Oscillator strengths and photoionization cross sections

The oscillator strengths for dipole-allowed transitions originating in the 2σ orbital of the ground state and ending in the npσ and npπ Rydberg states of CaH have been obtained with MQDO methodology. In these calculations, we have used the presently determined adiabatic ionization potential and vertical excitation energies. The present absorption oscillator strengths are collected in Table 3. Comparative data reported by Bruna and Grein [18] and by Barbuy et al.[17] also have been included. Bruna and Grein [18] carried out *ab initio* calculations using multi-reference configuration interaction (MRDCI) wavefunctions. Barbuy et al. [17] have derived oscillator strengths from the spectra of cool dwarfs computed using model atmospheres. As can be seen in Table 3, there is a reasonable agreement between the MQDO f-values and the comparative ones for the $X^2\Sigma^+$-4pπ($A^2\Pi$) and $X^2\Sigma^+$-5pσ($K^2\Sigma^+$) transitions. We note that our *f*-value for the $X^2\Sigma^+$-5pπ($L^2\Pi$) transition is a factor of 10 lower than the value indicated by Bruna and Grein [18]. No comparative values on intensities corresponding to transitions to Rydberg states with n>5 seem to be available to date.

In this work, we also have calculated photoionization cross sections for the kpσ and kpπ dipole-allowed Rydberg channels arising from the excitation of the 2σ orbital of the ground state of CaH. The electronic partial cross sections for the photoionization of CaH from the outermost orbital have been determined by adding the cross sections corresponding to each of the single ionization channels, i.e. the 2σ-kpσ and 2σ-kpπ excitations. For the kpσ and kpπ Rydberg channels, we have adopted a quantum defect value of ~2.0. In Figure 2, the MQDO cross sections are plotted versus the photon energy up to an energy of 70 eV. According our calculations, the 2σ molecular orbital of CaH is basically a Ca 4s orbital. Given that the radial wave function of such an orbital has nodes, a change in sign of the radial dipole matrix element for both studied Rydberg channels is

found and, thus, a minimum is expected in the photoionization cross section profile. An inspection of Figure 2 reveals the presence of a Cooper minimum for each of the Rydberg channels at a photon energy of ~6.2 eV for kpσ and ~6.6 eV for kpπ. Thus, a minimum also is present in the electronic partial photoionization cross section at a photon energy of ~6.5 eV.

No comparative data appear to be available in the literature either for the electronic partial photoionization cross sections or for the two Rydberg ionization channels to test the accuracy of the present calculations. Given this lack of comparative data, we have evaluated the oscillator strength spectral density (df/dE) in the complete spectral region assuming that continuity through the threshold is expected for a given spectral series between the discrete and continuum region. In the discrete part of the spectrum, the oscillator strengths are represented in form of a histogram following the procedure developed by Fano and Cooper [40]. In the continuum region, the oscillator strength spectral density is derived from the calculated MQDO cross section through the following expression:

$$\sigma(E) = 1.098 \times 10^{-16}\,\mathrm{cm}^2\mathrm{eV}\left(\frac{df}{dE}\right)$$

In Figures 3 and 4 we display the MQDO oscillator strength spectral density for both the continuum and discrete regions of spectrum corresponding to excitations from the 2σ orbital to npσ and npπ with n=5-9 and the continuum. As can be seen in both Figures, continuity between spectral densities in the continuum and discrete region at the ionization potential is observed.

Conclusions

In the present work, vertical excitation energies for Rydberg states of CaH have been determined with electron-propagator methods. A large number of excited Rydberg states have been investigated and the results are consistent with the scarce experimental data. To the best of our knowledge, some of the highest-energy states we have calculated have never been the object of experimental or theoretical work. For the first time, Rydberg states of *f* character have been considered. Oscillator strengths and photoionization cross sections of CaH also have been calculated by using the MQDO approach. A Cooper minimum has been found for photoionization from the outermost electron of the ground state. Given the lack of comparative data, we take the continuity of the differential oscillator strength across the ionization threshold as an assessment of the adequacy of the MQDO approach for the calculation of spectral intensities. We expect that the data supplied by the present work will help in future analysis and interpretation of the electronic spectrum of CaH.

Acknowledgements

The authors at Auburn University acknowledge the support of the National Science Foundation through grant CHE-1565760 and useful discussions on the performance of the electron-propagator calculations with O. Dolgounitcheva and V. G. Zakrzewski. The authors at Valladolid University acknowledge the support of the Junta de Castilla y León (Project No. Va077U13).

References

[1] C. Olmsted, Astrophys. J. 27 (1908) 66.

[2] A. Eagle, Astrophys. J. 30 (1909) 231.

[3] A. Fowler, Proc. Roy. Soc. London A 79 (1907) 509.

[4] J.D. Kirkpatrick. An. Rev. Astron. Astrophys. 43 (2005) 195.

[5] A. Burrows, W.B. Hubbard and J.I. Lunine, J. Liebert, Rev. Mod. Phys. 73 (2001) 719.

[6] P. Sotirowski, Astron. Astrophys. Suppl. Ser. 6 (1972) 85.

[7] A.J. Burgasser, J.D. Kirkpatrick, J. Liebert and A. Burrows, Astroph. J. 594 (2003), 510.

[8] M. D. Di Rosa, European Phys. J.D. 31 (2004) 395.

[9] S. Sakamoto, F.J. White, K. Kawaguchi, M. Ohishi, K.S. Usuda and T. Hasegawa, Mon. Not. R. Astron. Soc. 301 (1988) 872.

[10] A. Burrows, W.B. Hubbard, J.I. Lunine and J. Liebert, Rev. Mod. Phys. 73 (2001) 719.

[11] J. Tennyson and S. N. Yurchenko, Mon. Not. R. Astron. Soc. 425 (2012) 21.

[12] A. Shayesteh, K.A. Walker, I. Gordon, D.R.T. Appadoo and P.F. Bernath, J. Mol. Struct. 695 (2004) 23.

[13] B. Yadin, T. Veness, P. Conti, C. Hill, S.N. Yurchenko and J. Tennyson, Mon. Not. R. Astron. Soc. 425 (2012) 34.

[14] J. V. Ortiz, WIREs Comput. Mol. Sci. 3 (2013) 123.

[15] H. H. Corzo and J. V. Ortiz, Adv. Quantum Chem., in press.

[16] P.F. Week, P.C. Stancil and K. Kirby, J. Chem. Phys. 118 (2003) 9997.

[17] C. Barbuy, R.P. Schiavon, J. Gregorio-Hetem, P.D. Singh and C. Batalha, Astron. Astrophys. Suppl. Ser. 101 (1993) 409.

[18] P.J. Bruna and F. Grein, Phys. Chem. Chem. Phys. 2 (2003) 3140.

[19] I. Martín, A.M. Velasco, C. Lavín, E. Olaya and E. Bustos, Int. J. Quantum Chem. 85 (2001) 345.

[20] C. Lavín and A.M. Velasco, J. Quant. Spectrosc. Rad. Transfer 127 (2013) 96.

[21] A.M. Velasco, C. Lavín C, I. Martín, J. Pitarch-Ruiz and J. Sánchez-Marín, Chem. Phys. Lett. 462 (2008) 344.

[22] J.V. Ortiz, I. Martín, A.M. Velasco and C. Lavín, J. Chem. Phys. 120 (2004), 7949.

[23] J. Melin, J.V. Ortiz, I. Martín, A.M. Velasco and C. Lavín, J. Chem.Phys. 122 (2005) 234317.

[24] T.A. Carlson, M.O. Krause, W.A. Svensson, P. Gerard, F.A. Grimm, T.A. Whithley and B.P. Pullen, Z. Phys. D: At. Mol. Clusters 2 (1986) 309.

[25] A.M. Velasco, C. Lavín, O. Dolgounitcheva, J.V. Ortiz, J. Chem. Phys. 141 (2014) 074308.

[26] A.M. Velasco, C. Lavín, I. Martín, J. Melin, J.V. Ortiz, J. Chem. Phys. 131 (2009) 024104.

[27] T.H. Dunning, J. Chem. Phys. 90 (1989) 1007.

[28] J. Koput and K.A. Peterson, J. Phys. Chem. A, 106 (2002) 9595.

[29] K. Raghavachari, G. W. Trucks, J. A. Pople and M. Head-Gordon, Chem. Phys. Lett. 157 (1989) 479-483.

[30] Gaussian Development Version, Revision I.03, M. J. Frisch, G. W. Trucks, H. B. Schlegel, G. E. Scuseria, M. A. Robb, J. R. Cheeseman, G. Scalmani, V. Barone, B. Mennucci, G. A. Petersson, H. Nakatsuji, M. Caricato, X. Li, H. P. Hratchian, J. Bloino, B. G. Janesko, A. F. Izmaylov, A. Marenich, F. Lipparini, G. Zheng, J. L. Sonnenberg, W. Liang, M. Hada, M. Ehara, K. Toyota, R. Fukuda, J. Hasegawa, M. Ishida, T. Nakajima, Y. Honda, O. Kitao, H. Nakai, T. Vreven, K. Throssell, J. A. Montgomery, Jr., J. E. Peralta, F. Ogliaro, M. Bearpark, J. J. Heyd, E. Brothers, K. N. Kudin, V. N. Staroverov, T. Keith, R. Kobayashi, J. Normand, K. Raghavachari, A. Rendell, J. C. Burant, S. S. Iyengar, J. Tomasi, M. Cossi, N. Rega, J. M. Millam, M. Klene, J. E. Knox, J. B. Cross, V. Bakken, C. Adamo, J. Jaramillo, R. Gomperts, R. E. Stratmann,

O. Yazyev, A. J. Austin, R. Cammi, C. Pomelli, J. W. Ochterski, R. L. Martin, K. Morokuma, V. G. Zakrzewski, G. A. Voth, P. Salvador, J. J. Dannenberg, S. Dapprich, P. V. Parandekar, N. J. Mayhall, A. D. Daniels, O. Farkas, J. B. Foresman, J. V. Ortiz, J. Cioslowski, and D. J. Fox, Gaussian, Inc., Wallingford CT, 2014.

[31] I. Martín, Y. Pérez-Delgado and C. Lavín, Chem. Phys. Lett. 305 (1999) 178.

[32] A.M. Velasco, E. Mayor and I. Martín, Chem. Phys. Lett. 377 (2003) 189.

[33] B. Kaving and B. Lindgren, Phys. Scripta 10 (1974) 81.

[34] NIST Atomic Spectra Database , http://physics.nist.gov/asd3, National Institute of Standards and Technology, Gaithersburg, MD.

[35] K.P. Huber and G. Herzberg, Molecular Spectra and Molecular Structure, vol. 4. Constants of Diatomic Molecules, Van Nostrand Reinhold, New York, 1979.

[36] A. Shayesteh, R. S. Ram and P. F. Bernath, J. Mol. Spectrosc. 288 (2013) 46.

[37] R.S. Ram, K. Tereszchuk , I.E. Gordon , K.A. Walker and P.F. Bernath , J. Mol. Spectrosc. 266 (2011) 86.

[38] T. Leininger and G.-H. Jeung, J. Chem. Phys. 103 (1995) 3942.

[39] M. Aslam Khan, Proc. Phys. Soc. 80 (1962) 593.

[40] U. Fano and J.W. Cooper, Rev. Mod. Phys. 40 (1968) 441.

Table 1. Vertical excitation energies (eV) of CaH

MO[a]	Δ_{3+}[b]	P[c]	IR[d]	Q[e]	MO[a]	Δ_{3+}[b]	P[c]	IR[d]	Q[e]
6	0.000	0.97	σ	4s	52	5.173	1.00	σ	0.48d[f]
7	1.792	0.97	π	4p	53	5.176	1.00	π	0.57d, 0.31p
9	2.017	0.96	σ	0.59d, 0.34p	55	5.239	1.00	σ	8s
10	2.461	0.95	δ	3d	56	5.185	1.00	φ	f
12	2.696	0.93	π	d	58	5.293	0.99	π	8p
14	3.510	0.99	σ	5s	60	5.191	1.00	δ	f
15	4.057	0.99	π	5p	62	5.293	1.00	σ	0.53p, 35f
17	4.066	0.98	σ	0.54p, 0.34d	63	5.202	0.97	π	f
18	4.250	0.99	δ	4d	65	5.203	1.00	σ	0.57f, 0.30p
20	4.353	0.98	σ	0.53d, 0.24p	66	5.351	1.00	δ	7d
21	4.375	0.99	π	d	68	5.353	1.00	σ	d
23	4.561	1.00	σ	6s	69	5.355	1.00	π	d
24	4.783	1.00	φ	f	71	5.401	1.00	σ	9s
26	4.781	0.99	π	6p	72	5.425	0.98	π	9p
28	4.826	1.00	δ	f	74	5.426	1.00	σ	p
30	4.776	0.99	σ	0.53p, 0.29d	75	5.469	1.00	σ	d
31	4.853	1.00	π	f	76	5.470	1.00	δ	8d
33	4.860	1.00	σ	f	78	5.483	0.48	π	d
34	4.863	1.00	δ	5d	78	5.468	0.82	π	d
36	4.911	0.99	σ	0.42d[f]	80	5.507	1.00	σ	10s
37	4.919	1.00	π	0.52d, 0.34p	81	5.522	0.99	π	10p
39	4.998	1.00	σ	7s	83	5.522	1.00	σ	p
40	5.103	1.00	φ	f	84	5.520	1.00	σ	d
42	5.109	0.98	π	7p	85	5.521	1.00	δ	9d
44	5.124	1.00	δ	f	87	5.520	0.98	π	d
46	5.104	1.00	σ	0.51p, 0.24f	89	5.572	1.00	σ	11s
47	5.266	0.09	π	f	90	5.582	1.00	π	11p
47	5.137	0.97	π	f	92	5.582	1.00	σ	p
49	5.145	1.00	σ	0.48f, 0.45d	93	5.504	0.99	σ	0.59d, 0.39f
50	5.162	1.00	δ	6d	94	5.612	1.00	σ	12s

[a] Dominant canonical Hartree-Fock orbital component in Dyson orbital. Five occupied molecular orbitals (1σ + Ca 3s, $3p_x$, $3p_y$ and $3p_z$) are included in the 3+ calculations of the electron affinities of CaH^+. Molecular orbital 6 = 2σ.

[b] Excitation energy = difference between electron affinities in 3+ electron-propagator calculations

[c] Pole strength (norm of Dyson orbital for electron affinity)

[d] Irreducible representation

[e] Dyson orbitals' dominant (> 0.6) Ca atomic character or s, p, d and f Mulliken charges for mixed cases; n quantum numbers are given for nsσ, npπ and ndδ Rydberg series.

[f] For MO=36: 0.42d, 0.28p, 0.27f. For MO=52: 0.48d, 0.24p, 0.24f

Table 2. Vertical excitation energies (eV) of CaH

This work		Expt.[a]	
	ΔE		T_e
$4p\pi(^2\Pi)$	1.792	$A^2\Pi$ (4p)	1.786
$3d\sigma(^2\Sigma^+)$*	2.017	$B^2\Sigma^+$ (4p)	1.954
$3d\pi(^2\Pi)$	2.696	$E^2\Pi$	2.528
$5s\sigma(^2\Sigma^+)$	3.510	$C^2\Sigma^+$	3.51
$5p\pi(^2\Pi)$	4.057	$L^2\Pi$ (5p)	4.052
$5p\sigma(^2\Sigma^+)$*	4.066	$K^2\Sigma^+$ (5p)	4.05
$4d\delta\ (^2\Delta)$	4.250	$M^2\Delta$ (4d)	4.40
$4d\sigma(^2\Sigma^+)$*	4.353	$G^2\Sigma^+$ (4d)	4.31
$4d\pi(^2\Pi)$	4.375	$J^2\Pi$ (4d)	4.35
$6s\sigma(^2\Sigma^+)$	4.561	$F^2\Sigma^+$	4.55

[a]See [35] and [36] (A and B states) , [37] (E state)

*mixed orbital

Table 3. Oscillator strengths for transitions from the ground state to npπ and npσ Rydberg series of CaH

Transition	MQDO[a]	Comparative
$X^2\Sigma^+$ - 4pπ($^2\Pi$)	0.3666	0.39[b], 0.55[c]
$X^2\Sigma^+$ - 5pπ($^2\Pi$)	0.00074	0.03[b]
$X^2\Sigma^+$ - 6pπ($^2\Pi$)	0.00065	
$X^2\Sigma^+$ - 7pπ($^2\Pi$)	0.00018	
$X^2\Sigma^+$ - 8pπ($^2\Pi$)	0.00007	
$X^2\Sigma^+$ - 9pπ($^2\Pi$)	0.00003	
$X^2\Sigma^+$ - 5pσ($^2\Sigma^+$)	0.00055	0.0003[b]
$X^2\Sigma^+$ - 6pσ($^2\Sigma^+$)	0.00022	
$X^2\Sigma^+$ - 7pσ($^2\Sigma^+$)	0.00005	
$X^2\Sigma^+$ - 8pσ($^2\Sigma^+$)	0.00002	
$X^2\Sigma^+$ - 9pσ($^2\Sigma^+$)	0.00001	

[a] This work
[b] Bruna and Grein
[c] Barbuy et al.

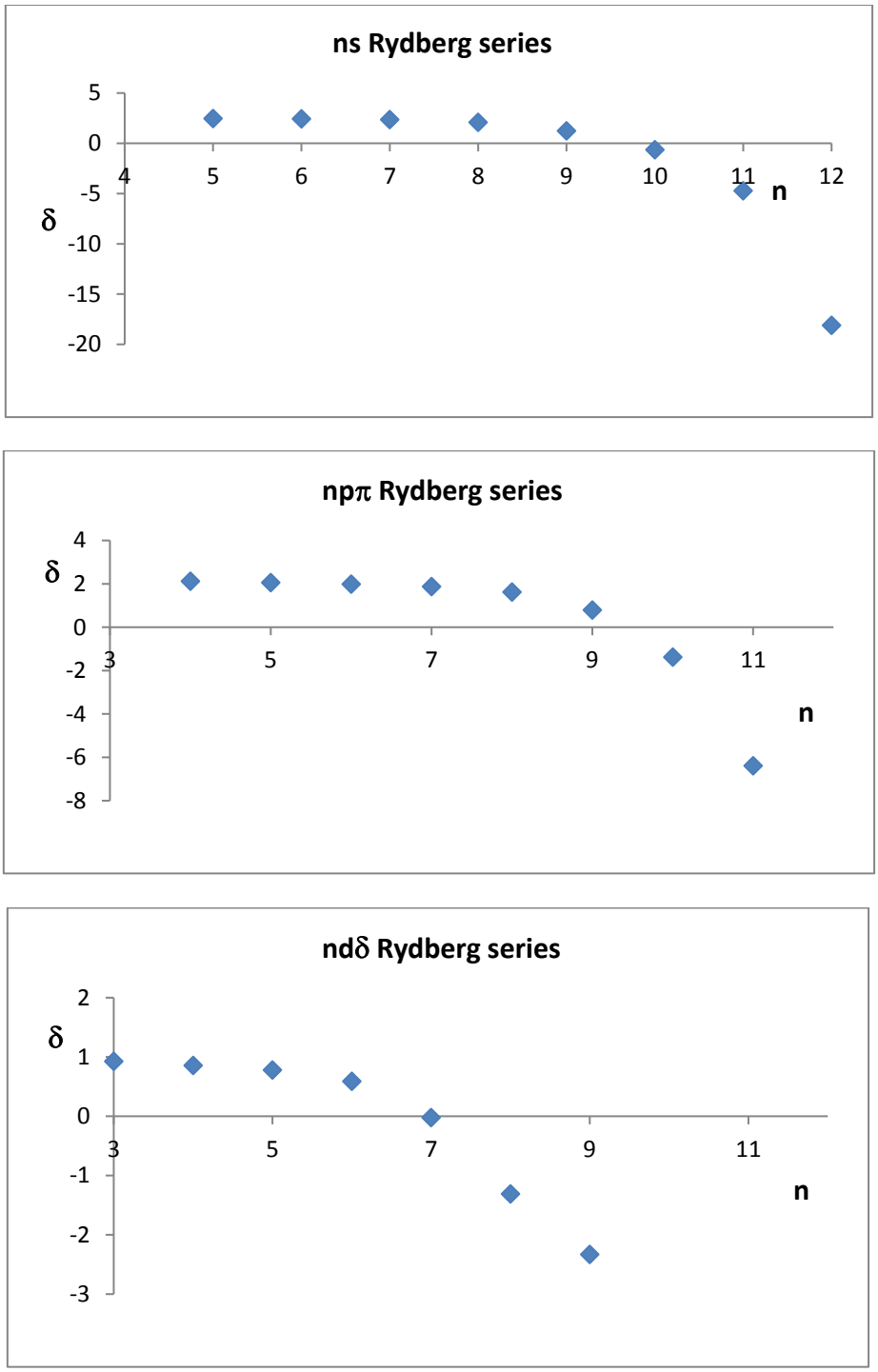

Figure 1. Calculated quantum defects (δ) versus principal quantum number (n) for nsσ, npπ and ndδ Rydberg series.

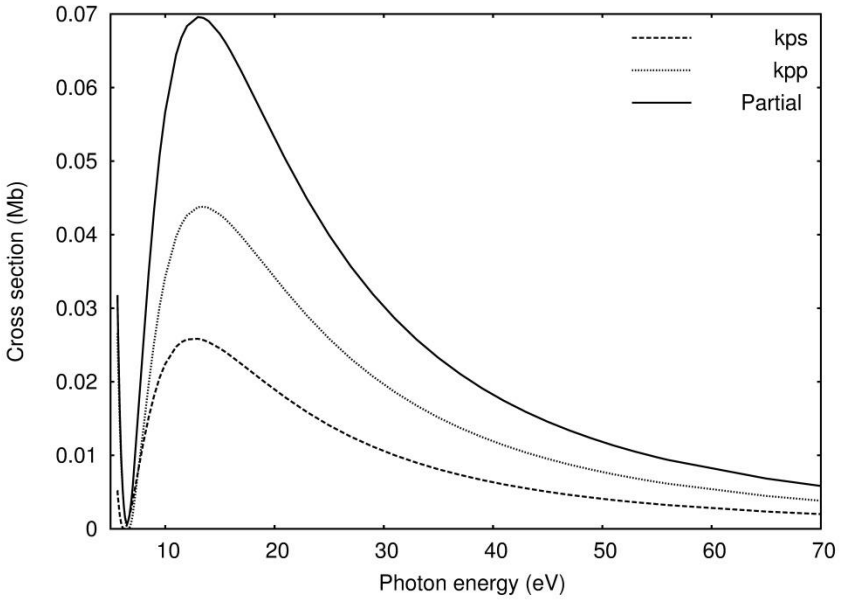

Figure 2. MQDO partial and individual cross sections profiles for the Rydberg channels that arise from the 2σ molecular orbital of CaH in its ground state.

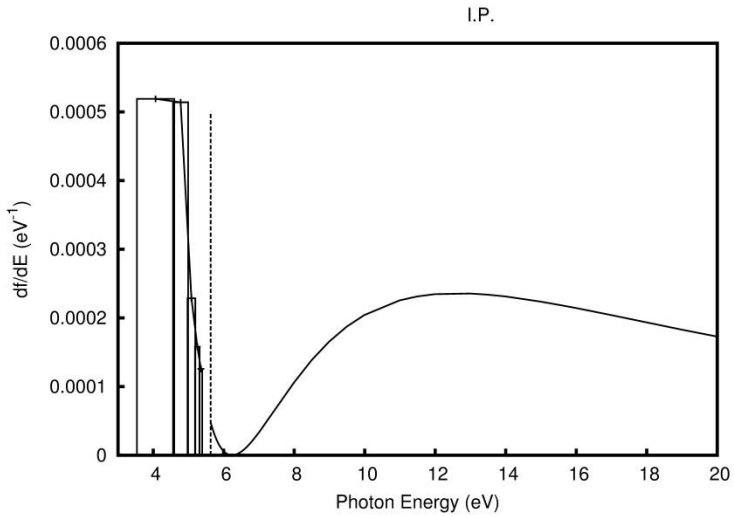

Figure 3. MQDO oscillator strength spectral density for bound and continuum spectral regions of the $X^2\Sigma^+$ - npσ($^2\Sigma^+$) (n=5-9, continuum) Rydberg series of CaH as a function of photon energy.

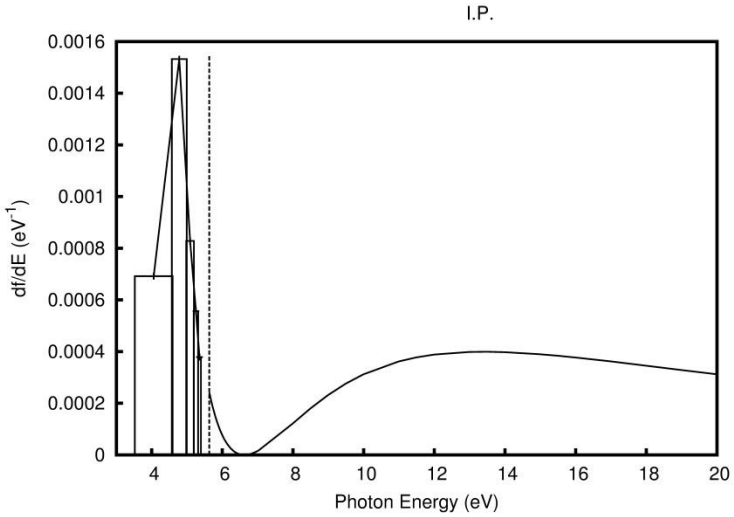

Figure 4. MQDO oscillator strength spectral density for bound and continuum spectral regions of the $X^2\Sigma^+$ - $np\pi(^2\Pi)$ (n=5-9, continuum) Rydberg series of CaH as a function of photon energy.